FOCUS REVIEW

Development of highly functional membranes through structural control of crystalline/amorphous phases

Hiroki Uehara[1]

Abstract

Molecular entanglements have been thought to restrict a desirable chain orientation during drawing. Therefore, a reduction in chain entanglements has been a focus for manufacturing high-performance fibers and membranes. In contrast, our melt-drawing technique utilizes molecular entanglements as a strain transmitter, achieving a nanoperiodic arrangement in which the crystalline and amorphous phases are interconnected. This periodic structure is similar to microphase separation in block copolymers, in which linked points are located at the boundaries between chemically different phases. The results show highly functional membranes can be successfully prepared from highly entangled homopolymer, as well as block copolymer, using solvent-free procedures.

Introduction

Polymeric molecules consist of the linear propagation of strong covalent bonds along the chain direction, but the lateral arrangement exhibits only weak van der Waals interactions. Therefore, drawing polymeric materials involves the anisotropy of various physical properties, including mechanical strength and optical polarity. Another feature of polymeric molecules is entanglement within one chain or between adjacent chains, which reduces the crystallinity of the material, imparting flexibility and transparency. These molecular entanglements often restrict the introduction of molecular anisotropy; thus, disentanglement has been a focus for manufacturing high-performance fibers and membranes with high crystallinity in the polymer processing field. In contrast, our "melt-drawing" technique [1–10] utilizes molecular entanglements as the strain transmitter, leading to oriented crystallization. Such molecular entanglements divide the crystalline and amorphous phases, which are similar to the linked points causing microphase separation in block copolymer [11]. Melt-drawing techniques also achieve the periodic arrangement

of these phases [12], which replaces the paradigm from conventional "entanglement exclusion for high performance" into novel "entanglement utilization for high functionality". In this review, our recent developments for nanostructured membranes using block copolymers and homopolymers are compared and reviewed based on their structural similarities.

Nanoporous membrane preparation from block copolymer

Block copolymer exhibits various beautiful nanoperiodic structures, the so-called "microphase separation", at the nanometer scale, which often exhibit high performance or function through later chemical modifications [13]. In this study, a simple diblock copolymer consisting of typical crystalline polyethylene (PE) and amorphous polystyrene (PS) segments (PE-*b*-PS) was selected. Purified powder of PE-*b*-PS was dissolved in hot *p*-xylene, and the solution was cast and dried into the film. Subsequent melt-recrystallization under optimum conditions gave the characteristic bicontinuous phase arrangements of crystalline and amorphous phases. This film was further treated with fuming nitric acid, which selectively etches the amorphous phase. The resultant nanoporous PE membrane contains network pore channels with 30 nm diameter, which pass across a membrane thickness of a few tens of microns (Fig. 1a). The pore size is significantly uniform due to

✉ Hiroki Uehara
  hirokiuehara@gunma-u.ac.jp

[1] Division of Molecular Science, Faculty of Science and
  Technology, Gunma University, Kiryu, Gunma 376-8515, Japan

Fig. 1 Appearance of nanoporous PE membrane prepared from PE-*b*-PS precursor film. Scanning electron microscope (SEM) images of the membrane surface (**a**) and photograph of the bent membrane (**b**). Adapted with permission [13]. Copyright © 2006 American Chemical Society
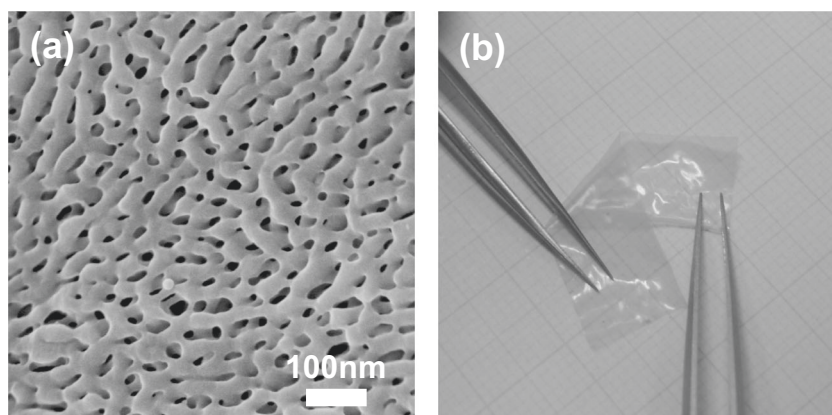
periodic phase separation of the precursor crystalline/amorphous arrangement of PE-*b*-PS.

Nanoporous networks are spread over the membrane surface with an area of 60 cm^2, indicating that practical filtration or permeation is applicable. Indeed, the gas permeation coefficient of this nanoporous membrane was 1.4 times larger than that of the commercial lithium-ion battery separator. The average surface area estimated by the BET (Brunauer–Emmett–Teller) method [14] using nitrogen gas was 17 m^2/g, corresponding to approximately half of the theoretical value for nanoporous ceramics prepared from the block copolymer precursor [15]. Another advantage lies in its flexibility attributed to the PE component, which is required for various membrane applications. Such membrane flexibility successfully prevents breaking even when bent or rolled (Fig. 1b). In addition, the tensile strength reached 30 MPa, which is similar to the above commercial lithium-ion battery separator. A characteristic network structure composed of crystalline PE component achieves desirable membrane robustness.

## Nanoporous polyethylene membrane for implantable glucose sensor application

A narrower distribution of pore size in the above nanoporous PE membrane is preferable for the size-selective separation of targeted solute [16], e.g., dialyzer excluding glucose molecule. Recently, glucose sensing technology has become necessary in healthcare due to a rapid increase in diabetic patients, especially in developed countries, including Japan. Conventional glucose sensing is widely achieved using daily blood tests, which restricts quality of life of patients. Implantable glucose sensors [17, 18] could be a possible solution, but their practical use requires downsizing the sensing components, including microelectromechanical system (MEMS) technology. The robustness of the abovementioned nanoporous PE membrane is suitable for rolling, folding or bending applications [13], which

are preferable for MEMS design. Therefore, the glucose permeability of the nanoporous PE membrane was tested. Here, a series of membranes with different pore sizes from 5 to 40 nm was prepared by varying the etching conditions for the precursor PE-*b*-PS membrane with bicontinuous crystalline/amorphous phases [13, 16, 19]. Albumin permeation was also compared to confirm the size-selective permeation of these membranes. All of the etched membranes permeate the glucose molecules, but the membranes with pores smaller than 10 nm perfectly block the permeation of albumin molecules larger than glucose molecules (Fig. 2a). In contrast, the commercialized alumina nanoporous membrane exhibits an unavoidable leak of albumin molecules (Fig. 2b), indicating the significant advantage of the targeted nanoporous PE membranes. These results were obtained through international collaboration with the Swiss Federal Institute of Technology in Lausanne (EPFL).

Development of fuel-cell membrane with low water uptake and high ion conductivity

The abovementioned bicontinuous phase crystalline/amorphous phase arrangements of the PE-*b*-PS precursor film are also available for preparation of electrolyte membrane for fuel cells [20], which has been used as a key technology for reducing carbon-dioxide exhaust. In particular, its use in automobiles is becoming a social demand for a sustainable society. However, continuous vibration during driving might cause liquid spills, and thus an electrolyte membrane that can operate with less water content is highly desirable for automobile application. The abovementioned PE-*b*-PS precursor film was prepared by melt-recrystallization procedure under optimum conditions [13, 16]. Subsequent sulfonating treatment gives a characteristic nanostructured electrolyte membrane, where the proton conductive networks of sulfonated PS phases are supported by robust skeletons composed of crystalline PE phases (Fig. 3). Here, the latter skeleton phase restricts additional swelling of the

Fig. 2 Schematic illustrations of glucose (green dot) and albumin permeation (red spheres). Nanoporous PE membrane (**a**) and commercial alumina porous membrane (**b**). Adapted with permission [16]. Copyright © 2009 American Chemical Society
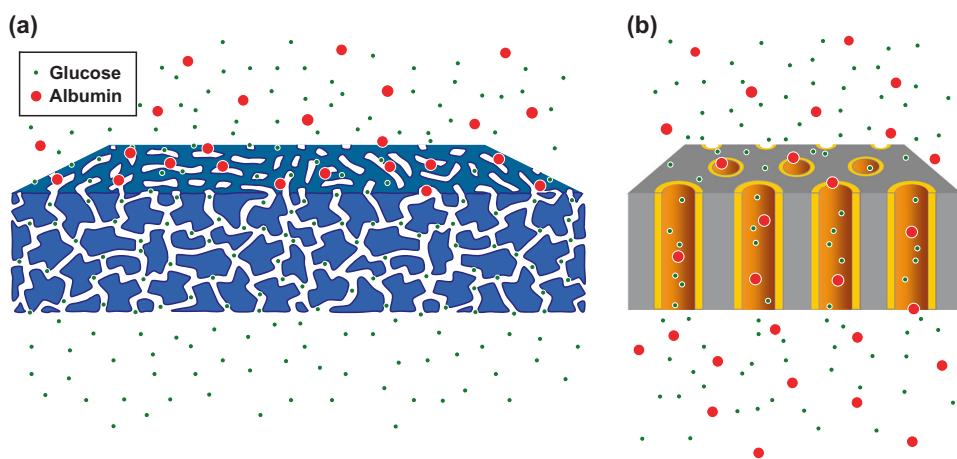
Fig. 3 Three-dimensional scanning electron microscope (3D SEM) image of the fuel-cell membrane composed of amorphous electrolyte channels (dark region) supported by a crystalline backbone network (bright region). Adapted with permission [20]. Copyright © 2009 American Chemical Society
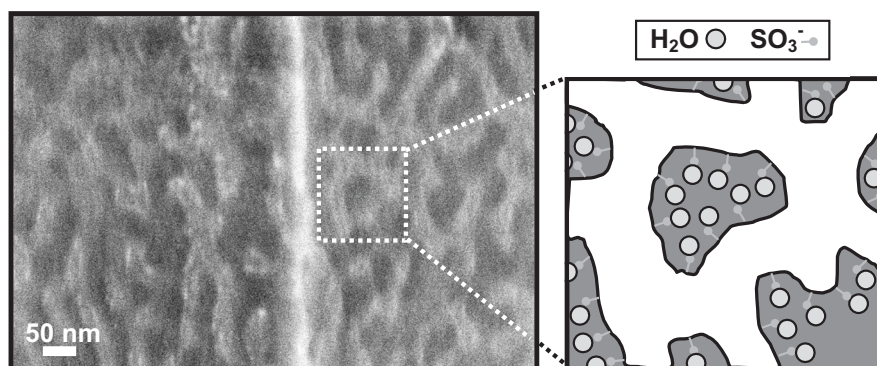

proton conductive phase, lowering the water content to 7 wt % but maintaining a similar proton conductivity of 0.09 S/cm compared to the state-of-the-art polymeric-electrolyte membrane of Nafion (30 wt% and 0.10 S/cm) [21–25]. Elemental analysis of our nanostructured membrane indicates that the number of water molecules trapped by a SO_3 group is only one, which is remarkably lower than the range of 10 to 30 for a Nafion membrane [21, 26]. Such perfect one-to-one pairing meets the conditions of low water content and high proton conductivity. This development of a polymeric-electrolyte membrane was achieved through collaboration with Toyota Motor Corp.

Nanoperiodic and nanoporous structural formation of ultrahigh molecular weight polyethylene

As introduced above, the block copolymer provides an excellent nanostructured precursor, where both the crystalline and amorphous phases are interconnected. However, one disadvantage lies in the high cost of preparing block copolymer, which requires precise control of the segment length to achieve the targeted microphase separation. In contrast,

conventional homopolymers are much cheaper, but usually exhibit typical crystalline and amorphous phases. Recently, we [12] have successfully prepared a nanoperiodic structure via arrangement control of molecular entanglements, even for homopolymers. The longest chain is preferred because it contains a large number of entanglements targeted for such nanostructural control. In addition, the simplest chemical architecture of PE promises to emphasize the capability of this processing technique compared to the synesthetic approach for precise segmental control of block copolymers. Therefore, we chose ultrahigh molecular weight polyethylene (UHMW-PE) with these molecular features, which is known as an engineering plastic. UHMW-PE film was prepared by solution casting and annealed above its melting temperature (T_m), followed by being uniaxially drawn and subsequently relaxed [27]. The resultant morphology exhibits a periodic arrangement of lamellar crystals 30 nm thick, as depicted in Fig. 4a. Three-dimensional rotating analysis in transmission electron microscopy allows us to propose a network model of crystalline lamellae (bright region), where the amorphous component (dark region) is also interconnected, as illustrated in Fig. 4c. Such a nanoperiodic structure is very similar to a bicontinuous crystalline/amorphous phase arrangement for the PE-*b*-PS precursor film in Fig. 4b [13, 16, 20]. In comparison

Fig. 4 Comparison of
nanostructured membranes
prepared in this study.
Nanoperiodic structure induced
by uniaxial drawing for
UHMW-PE film (**a**) [12] and
bicontinuous structure
composed of crystalline/
amorphous phases for PE-*b*-PS
(**b**) [11]. Structural models of the
crystalline network for UHMW-
PE (**c**) [12] and block copolymer
(**d**) [28] are also compared.
Adapted with permission [12].
Copyright © 2007 American
Chemical Society. Adapted with
permission [11]. Copyright
© 2006 Wiley Periodicals, Inc.
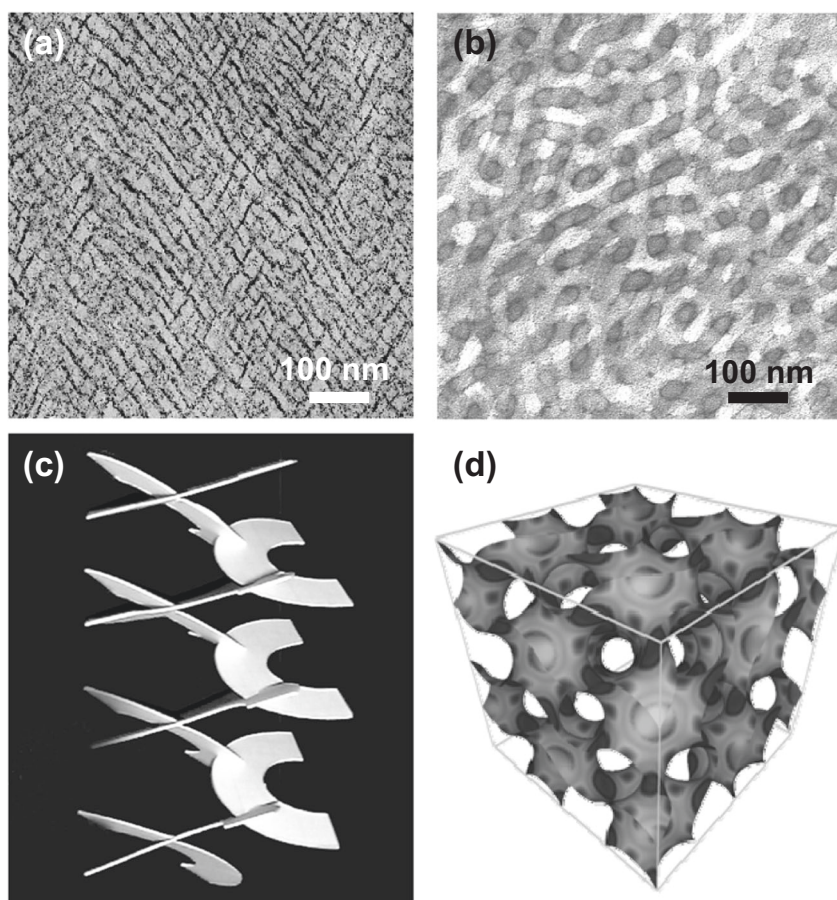
to the lamellar network model in Fig. 4c, the typical gyroid packing [28] of crystalline and amorphous phases for block copolymer is schematically depicted in Fig. 4d.

This lamellar thickness of drawn UHMW-PE is coincident with the rheologically estimated molecular weight between entanglements for PE (3500 Da) [29], indicating that entanglements are trapped on the crystalline surface. It is known that lamellar thickness depends on crystallization temperature for conventional PE with ~10^5 MW [30]. In contrast, UHMW-PE with MW above ~10^6 gives constant crystallinity at ~50% and at a T_m of 136 °C, independent of crystallization conditions, i.e., quenching, slow cooling or isothermal crystallization after melting [1]. These thermodynamic properties are also independent of MW in the range from 10^6 to 10^7 [5, 6, 10, 31, 32]. However, the origin of such constant thermodynamic properties of UHMW-PE has been a mystery. When this T_m is applied to the Thomson–Gibbs equation, representing the relationship between T_m and lamellar thickness [30], the coincident lamellar thickness is 30 nm, which agrees well with that estimated in Fig. 4a. Further, the same 30 nm has been reported as the maximum lamellar thickness of conventional PE with MW ~10^5 when crystallized at the highest temperature of 120 °C for 24 h [33].
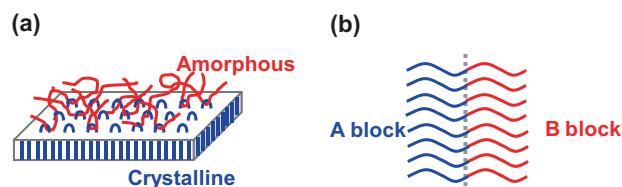
Fig. 5 Comparison of crystalline/amorphous phase arrangements of homopolymer and block copolymer. Boundaries between crystalline and amorphous phases are determined by arrangements of entanglements in homopolymer (**a**) and linked points in block copolymer (**b**). Adapted with permission [27]. Copyright © 2012 Wiley-VCH Verlag GmbH & Co. KGaA, Weinheim
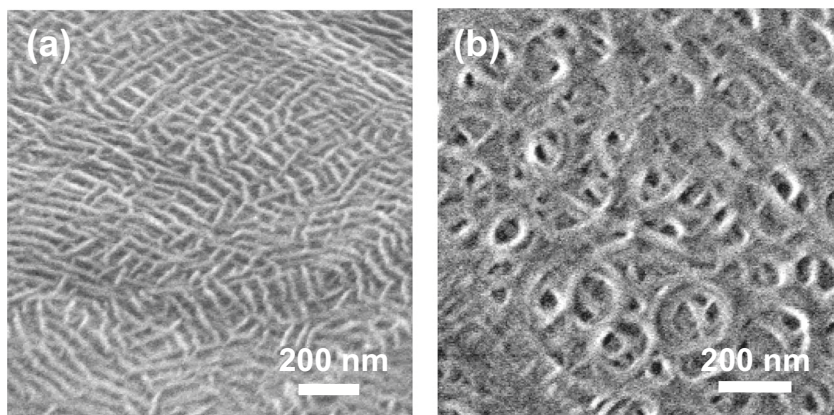
These duplicated coincidences suggest that the molecular entanglements in conventional polymer and linked points in block copolymers have similar roles in morphological formation, as schematically illustrated in Fig. 5. Here, the entanglements are trapped on the lamellar surface of the prepared UHMW-PE film. Molecular segments cannot travel beyond such trapped entanglements, leading to periodic arrangements of crystalline and amorphous phases, such as microphase separation in block copolymer.

The negligible difference between segmented linked points in block copolymer and molecular entanglements in UHMW-PE is attributed to their ability of positional
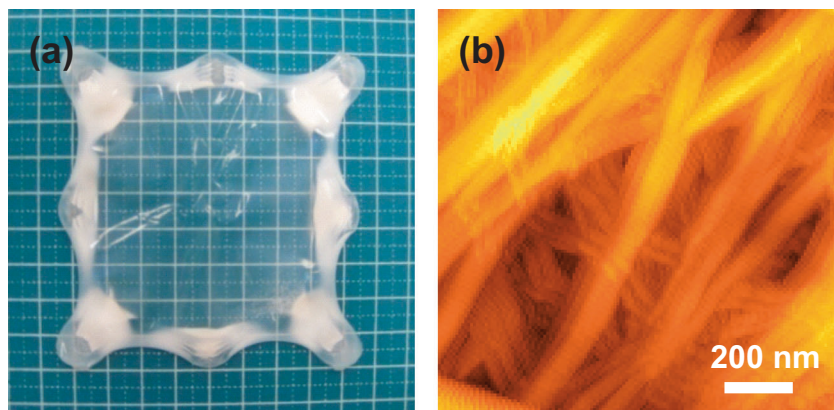
rearrangement. The position of the linked point in the former is fixed between different segments, but the latter molecular entanglements can slide along the chain. The possible movement of molecular entanglements allows rearrangement of their position. To form the periodic arrangement in Fig. 4a, the drawing procedure effectively induces the sliding of molecular entanglements, which averages the resultant lamellar thickness, leading to a significantly sharp endotherm in the differential scanning calorimetry scan for drawn UHMW-PE [27].

The development of such periodic lamellar arrangements within the membrane was also tested for various industrial applications, including packaging or selective permeation. The combination of biaxial drawing and subsequent relaxing above the T_m of UHMW-PE gave periodic arrangements of lamellae with a constant thickness of 30 nm, which were spread over the membrane surface and across the membrane thickness, as depicted in Fig. 6a [27, 34, 35]. Such a membrane containing periodic lamellar arrangements was further biaxially drawn to contain nanopores formed by exfoliation between the lamellar crystals. The resultant redrawn membrane exhibits a network of nanopores, with a diameter of a few tens of nm, as depicted in Fig. 6b. This pore size is smaller than the state-of-the-art porous UHMW-PE membrane for an industrial lithium-ion battery separator.

Nanostructured membrane preparation for fluoropolymers

A similar method for nanostructured membrane manufacturing by biaxial drawing has been successfully achieved for fluoropolymers, including poly(tetrafluoroethylene) (PTFE) [36]. PTFE has various superior characteristics, including weather resistance, thermal stability and water repellency, which are preferable in roofing material. High mechanical strength is also required for membrane structure, e.g., for a dome roof, but the conventional compression molding for PTFE gives a brittle membrane. Therefore, glass fibers were composited with PTFE raw powder into the commercialized membrane of dome roofs. However, the boundaries between the glass fibers and PTFE matrix lead to redundant light scattering due to the difference in their reflective indexes, causing an opaque appearance in the manufactured membrane. Here, we [37] have focused on the higher melt-viscosity of PTFE, similar to UHMW-PE, which enables uniaxial melt-drawing into a robust film. This melt-drawing technique is successfully extended into biaxial directions to give the transparent PTFE membrane, as depicted in Fig. 7a. Such a biaxially melt-drawn PTFE membrane contains both extended-chain crystals (ECCs) and a residual lamellar matrix (Fig. 7b), where the former

Fig. 6 UHMW-PE membrane morphologies prepared by solvent-free manufacturing. Homogeneous lamellar membrane (**a**) and nanoporous membrane (**b**). Adapted with permission [27]. Copyright © 2012 Wiley-VCH Verlag GmbH & Co. KGaA, Weinheim

Fig. 7 Appearance of the biaxially melt-drawn membrane of PTFE. Photograph of transparent membrane with an area of 90x90 mm^2 (**a**) [36] and scanning probe microscopy (SPM) image composed of ECC networks with a lamellar matrix (**b**). Adapted with permission [36]. Copyright © 2013 Wiley-VCH Verlag GmbH & Co. KGaA, Weinheim

ECCs play a role in the backbone of the latter lamellar matrix [36]. This result is similar to a conventional composite of PTFE and glass fiber, but the boundary is negligible because both components are the same PTFE. Transparency and robustness for a biaxially melt-drawn PTFE membrane enables the efficient utilization of sunlight as dome illumination or power generation for a solar cell. Further, a so-called "one-composite" with pure PTFE enhances recycling management compared to a conventional composite with glass fiber. A similar high-performance membrane is obtained by biaxial drawing for the ethylene-tetrafluoroethylene copolymer [38]. This membrane development of fluoropolymers was achieved through a collaboration with Asahi Glass Corp.

Perspective

The current pore formation for the commercial lithium-ion battery separator, which is composed of UHMW-PE, has been achieved by evaporation or extraction of organic solvents, which are preloaded for the initial gel-extrusion process. However, these solvents are known to be carcinogenic, and thus their use is strictly controlled. The necessary collection of the resulting exhaust increases the production cost of the separator. In contrast, the abovementioned nanopore formation induced only by drawing procedures is perfectly "solvent-free", which is a tremendous advantage in the industrial manufacturing of the battery separator. In addition, this solvent-free manufacturing allows filtration for water purification, dialysis or other medical applications. These applications require further increases in pore volume and decreases in pore size, often leading to a conflict between these two factors in conventional solvent-assisted pore formation, e.g., for a battery separator. In contrast, our solvent-free technique enables a unique network of nanopores based on controlled arrangement of molecular entanglements, which possibly satisfies both requests in pore properties.

Compliance with ethical standards

References

1. Uehara H, Nakae, Kanamoto T, Zachariades AE, Porter RS. Melt drawability of ultra-high molecular weight polyethylene. Macromolecules. 1999;32:2761–9.
2. Nakae M, Uehara H, Kanamoto T, Ohama T, Porter RS. Melt drawing of ultra-high molecular weight polyethylene: comparison of Ziegler- and metallocene-catalyzed reactor powders. J Polym Sci Polym Phys Ed. 1999;37:1921–30.
3. Nakae M, Uehara H, Kanamoto T, Zachariades AE, Porter RS. Structure development upon melt drawing of ultra-high molecular weight polyethylene: effect of prior thermal history. Macromolecules. 2000;33:2632–41.
4. Uehara H, Kakiage M, Yamanobe T, Komoto T, Murakami S. Phase development mechanism during drawing from highly entangled polyethylene melts. Macromol Rapid Commun. 2006;27:966–70.
5. Kakiage M, Yamanobe T, Komoto T, Murakami S, Uehara H. Effects of molecular characteristics and processing conditions on melt-drawing behavior of ultra-high molecular weight polyethylene. J Polym Sci Polym Phys Ed. 2006;44:2455–67.
6. Kakiage M, Yamanobe T, Komoto T, Murakami S, Uehara H. Transient crystallization during drawing from ultra-high molecular weight polyethylene melts having different entanglement characteristics. Polym (Guildf). 2006;47:8053–60.
7. Uehara H, Yoshida R, Kakiage M, Yamanobe T, Komoto T. Continuous film processing from ultra-high molecular weight polyethylene reactor powder and mechanical property development by melt-drawing. Ind Eng Chem Res. 2006;45:7801–6.
8. Kakiage M, Sekiya M, Yamanobe T, Komoto T, Sasaki S, Murakami S, et al. In-situ SAXS analysis of extended-chain crystallization during melt-drawing of ultra-high molecular weight polyethylene. Polym (Guildf). 2007;48:7385–92.
9. Kakiage M, Sekiya M, Yamanobe T, Komoto T, Sasaki S, Murakami S, et al. Phase transitions during heating of melt-drawn ultra-high molecular weight polyethylenes having different molecular characteristics. J Phys Chem B. 2008;112:5311–6.
10. Kakiage M, Uehara H, Yamanobe T, Novel In-Situ NMR. Measurement system for evaluating molecular mobility during drawing from highly entangled polyethylene melts. Macromol Rapid Commun. 2008;29:1571–6.
11. Uehara H, Yoshida T, Kakiage M, Yamanobe T, Komoto T. Structural arrangement of crystalline/amorphous phases of poly-ethylene-*block*-polystyrene copolymer as induced by orientationtechniques. J Polym Sci Polym Phys Ed. 2006;44:1731–7.
12. Uehara H, Takeuchi K, Kakiage M, Yamanobe T, Komoto T. Nano-periodic arrangement of crystal/amorphous phases induced by tensile drawing of highly entangled polyethylene. Macromolecules. 2007;40:5820–6.
13. Uehara H, Yoshida T, Kakiage M, Yamanobe T, Komoto T, Nomura K, et al. Nanoporous polyethylene film prepared from bicontinuous crystalline/amorphous structure of block copolymer precursor. Macromolecules. 2006;39:3971–4.
14. Brunauer S, Emmett PH, Teller E. Adsorption of gases in multimolecular layers. J Am Chem Soc. 1938;60:309–19.
15. Chan VZH, Hoffman J, Lee VY, Iatrou H, Avgeropoulos A, Hadjichristidis N, et al. Ordered bicontinuous nanoporous and

nanorelief ceramic films from self assembling polymer precursors. Science. 1999;286:1716–9.

16. Uehara H, Kakiage M, Sekiya M, Sakuma D, Yamanobe T, Takano N, et al. Size-selective diffusion in nanoporous but flexible membranes for glucose sensors. ACS Nano. 2009;3:924–32.

17. Moscone D, Pasini M, Mascini M. Subcutaneous microdialysis probe coupled with glucose biosensor for in vivo continuous monitoring. Talanta. 1992;39:1039–44.

18. Ballerstadt R, Polak A, Beuhler A, Frye J. In vitro long-term performance study of a near-infrared fluorescence affinity sensor for glucose monitoring. Biosens Bioelectron. 2004;19:905–14.

19. Uehara H, Kano M, Tanaka H, Kato S, Masunaga H, Yamanobe T. Nanoporous morphology control of polyethylene membranes by block copolymer blends. RSC Adv. 2014;4:42467–77.

20. Uehara H, Kakiage M, Sekiya M, Yamagishi T, Yamanobe T, Nakajima K, et al. Novel design solving the conductivity vs water-uptake trade-off for polymer electrolyte membrane by bicontinuous crystalline/amorphous morphology of block copolymer. Macromolecules. 2009;42:7627–30.

21. Mauritz KA, Moore RB. State of understanding of nafion. Chem Rev. 2004;104:4535–86.

22. Kim M-H, Glinka CJ, Grot SA, Grot WG. SANS study of the effects of water vapor sorption on the nanoscale structure of perfluorinated sulfonic acid (NAFION) membranes. Macromolecules. 2006;39:4775–87.

23. Schmidt-Rohr K, Chen Q. Parallel cylindrical water nanochannels in nafion fuel-cell membranes. Nat Mater. 2008;7:75–83.

24. Majsztrik P, Bocarsly A, Benziger J. Water permeation through nafion membranes: the role of water activity. J Phys Chem B. 2008;112:16280–9.

25. Spry DB, Goun A, Glusac K, Moilanen DE, Fayer MD. Proton transport and the water environment in nafion fuel cell membranes and AOT reverse micelles. J Am Chem Soc. 2007;129:8122–30.

26. Cui S, Liu J, Selvan ME, Paddison SJ, Keffer DJ, Edwards BJ. Comparison of the hydration and diffusion of protons in perfluorosulfonic acid membranes with molecular dynamics simulations. J Phys Chem B. 2008;112:13273–84.

27. Uehara H, Tamura T, Kakiage M, Yamanobe T. Nanowrinkled and nanorporous polyethylene membrane via entanglement arrangement control. Adv Funct Mater. 2012;22:2048–57.

28. Gyroid structure, https://commons.wikimedia.org/wiki/File: Gyroid_surface_with_Gaussian_curvature.png

29. Graessley WW. The entanglement concept in polymer rheology. Adv Polym Sci. 1974;16:1–179.

30. Wunderlich, B. Macromolecular physics. New York: Academic Press; 1976.

31. Suwa J, Kakiage M, Yamanobe T, Komoto T, Uehara H. Molecular weight segregation on surfaces of polyethylene blended films as estimated from nanoscratch tests using scanning probe microscopy. Langmuir. 2007;23:5882–5.

32. Kato S, Tanaka H, Yamanobe T, Uehara H. In situ analysis for melt-drawing behavior of ultra-high molecular weight polyethylene films with different molecular weights: roles of entanglements on oriented crystallization. J Phys Chem B. 2015;119:5062–70.

33. Matsuda H, Aoike T, Uehara H, Yamanobe T, Komoto T. Crystalline surface free energy of linear polyethylene as estimated from a combination of crystal thickness distribution and DSC melting curve shapes. Kobunshi Ronbunshu. 2001;58:326–31.

34. Uehara H, Tamura T, Hashidume K, Tanaka H, Yamanobe T. Non-solvent processing for robust but thin membrane of ultrahigh molecular weight polyethylene. J Mater Chem A. 2014;2:5252–7.

35. Uehara H, Tamura T, Yamashita H, Yamanobe T, Masunaga H. Phase transition during heating of nanostructured ultra-high molecular weight polyethylene membrane. J Phys Chem B. 2015;119:15909–18.

36. Uehara H, Arase Y, Suzuki K, Yukawa Y, Higuchi Y, Matsuoka Y, et al. Highly transparent and robust poly(tetrafluoroethylene) membrane prepared by biaxial melt-drawing. Macromol Mater Eng. 2014;299:669–73.

37. Morioka T, Kakiage M, Yamanobe T, Komoto T, Kamiya H, Higuchi Y, et al. Oriented crystallization from poly(tetrafluoroethylene) melt induced by uniaxial drawing. Macromolecules. 2007;40:9413–9.

38. Uehara H, Ono Y, Kakiage M, Sakamura T, Masunaga H, Yukawa Y, et al. Property development for biaxial drawing of ethylene-tetrafluoroethylene copolymer films and resultant fractural behavior analyzed by in situ X-ray measurements. J Phys Chem B. 2015;119:4284–93.

Hiroki Uehara is a Professor of Division of Molecular Science, Faculty of Science and Technology, Gunma University. He received his B.Sci. and M.Sci. from the Tokyo University of Science (TUS) under the supervision of Professor Tetsuo Kanamoto and the research collaboration with Dr. Syozo Murakami in the Kyoto University. Thereafter, he worked as a visiting scientist at the University of Massachusetts at Amherst, USA, with late Emeritus Professor Roger S Porter and then received Ph.D. degrees from the TUS. Immediately, he moved to Gunma University as an Assistant Professor and worked with Professor Takeshi Yamanobe. His major interests are the control of molecular entanglements of ultrahigh molecular weight polymers and the fabrication of high-performance or high-functional materials via various processing technologies, including melt-drawing techniques. He received the Award for Encouragement of Research in Polymer Science; The Society of Polymer Science, Japan (SPSJ), in 1999, the Ichimura Prize in Science for Distinguished Achievement in 2010, the Yokoyama Award for Science and Technology in 2010, the Kurita Water and Environmental Research Award in 2011, the Award of the Society of Fiber Science and Technology, Japan, in 2017 and SPSJ Mitsubishi Chemical Award in 2017.